Pergamon

Tetrahedron 56 (2000) 955–964

TETRAHEDRON

Characterization of Self-Assembling Nano-Sized Structures by Means of Coldspray Ionization Mass Spectrometry

Shigeru Sakamoto,[a] Makoto Fujita,[b] Kimoon Kim[c] and Kentaro Yamaguchi[a,*]

[a]*Chemical Analysis Center, Chiba University, Yayoi-cho, Inage-ku, Chiba 263-8522, Japan*
[b]*Department of Applied Chemistry, School of Engineering, Nagoya University and CREST, Japan Science and Technology Corporation (JST), Chikusa-ku, Nagoya 464-8603, Japan*
[c]*Department of Chemistry, Pohang University of Science and Technology, San 31 Hyojadong, Pohang 790-784, South Korea*

Received 11 November 1999; accepted 13 December 1999

Abstract—Coldspray ionization (CSI) for mass spectrometry (MS) has been developed and applied to characterize labile self-assembling nano-sized metal complexes. While conventional ESI-MS is not applicable to these compounds because of their instability, CSI affords multiply charged molecular ions with many solvent (acetonitrile) molecules attached. We measured the exact mass of these molecular ions by using crown ether compounds as internal standards. Highly concentrated solutions (ca. 1 mmol/L) of the complexes, whose framework constitution is strongly influenced by concentration, could be used. In the case of some aqueous solutions, the molecular ions could be clearly observed by adjusting the temperature of the desolvation chamber to near the freezing point of water. This CSI-MS should be applicable to a wide variety of labile ionic compounds.

Introduction

Highly ordered supramolecules[1–14] such as catenanes, rotaxanes, molecular capsules and molecular necklaces, derived by self-assembly on transition metals, have unique structures and properties. Characterization of this class of metal complexes has generally been done with X-ray crystallography and NMR spectroscopy. However, it is often difficult to obtain a single crystal of sufficient quality for precise structure determination. Further, if molecules contain paramagnetic metals[10,14] and/or exhibit fast equilibration among plural structures,[15–17] NMR spectroscopy can provide only limited structural information. As regards mass spectrometry, these compounds are usually unstable to the ionization impact or matrix reagents, even in the case of mild ionization methods such as fast atom bombardment (FAB), matrix-assisted laser desorption ionization (MALDI) and electrospray ionization (ESI).[18–21] Even if the molecular ions are observed by using these ionization methods, many fragment ions also appear in the mass spectrum.[3,12–14]

Here we report a new method, coldspray ionization mass spectrometry (CSI-MS), which allows easy and precise characterization of labile self-assembling nano-sized structures in solution.

Keywords: mass spectrometry; catenanes; supramolecular chemistry; rotaxanes.

* Corresponding author. Tel.: +81-43-290-3810; fax: +81-43-290-3813; e-mail: yamaguchi@cac.chiba-u.ac.jp

Coldspray Ionization Mass Spectrometry (CSI-MS)

We have developed the CSI apparatus (Fig. 1), which consists of an electrospray (ESI) or ion spray (IS) ionization probe and a desolvation chamber operating at low temperature in order to detect unstable organometallic complexes.[22–24] It features a drying gas (N_2) cooling device to maintain the temperature of the capillary and spray itself below −20°C, in order to promote ionization based on increasing polarizability of the compounds caused by the higher dielectric constant at low temperature. The ion source block and the desolvation chamber are held at low temperature (−50 to 15°C) by pouring liquid nitrogen directly onto them, in order to allow transfer of unstable ions to the mass analyzer without decomposition. Mass

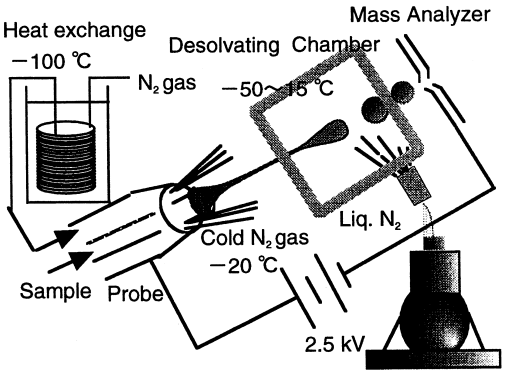

Figure 1. Schematic diagram of the coldspray ion source.

0040–4020/00/$ - see front matter
PII: S0040-4020(99)01092-3

spectral measurements were performed with a four-sector (BE/BE) tandem mass spectrometer (JMS-700T, JEOL) equipped with the CSI source.

Results and Discussion

Solvation in the CSI

In order to confirm the characteristics of this method, we carefully examined the solvation[25–27] observed in the CSI-MS of a small ionic molecule, cesium iodide (CsI). In the conventional ESI-MS spectrum of an acetonitrile (CH_3CN) solution of CsI, Cs^+ (m/z=133) and $[Cs+CH_3CN]^+$ (m/z=174) were observed (Fig. 2A). In the case of ionic metal complexes, molecular ions are formed based on electrolytic dissociation to the counter ions, driven by heat or solvation. Although Cs^+ and $[Cs+CH_3CN]^+$ formed by heat and solvation, respectively, were observed in conventional ESI-MS, $[Cs+CH_3CN]^+$ resulting from solvation was dominant in the CSI-MS spectrum (Fig. 2B). This suggests that coldspray may promote the dissociation of counter anions based on an increase of polarizability caused by the higher dielectric constant at low temperature. The dielectric polarization (**P**) is a function of vacuum permittivity (ϵ_0), relative permittivity or dielectric constant (ϵ_r) and electric field (**E**).

$$\mathbf{P} = \epsilon_0(\epsilon_r - 1)\mathbf{E} \quad (1)$$

Generally, higher dielectric constant of solvents is observed at low temperature, as described in Eq. (2) (T: temperature, θ: constant).

$$\epsilon_r = \epsilon_0 \, e^{-T/\theta} \quad (2)$$

Therefore, it should be possible to ionize thermally unstable ionic metal complexes by solvation without decomposition.

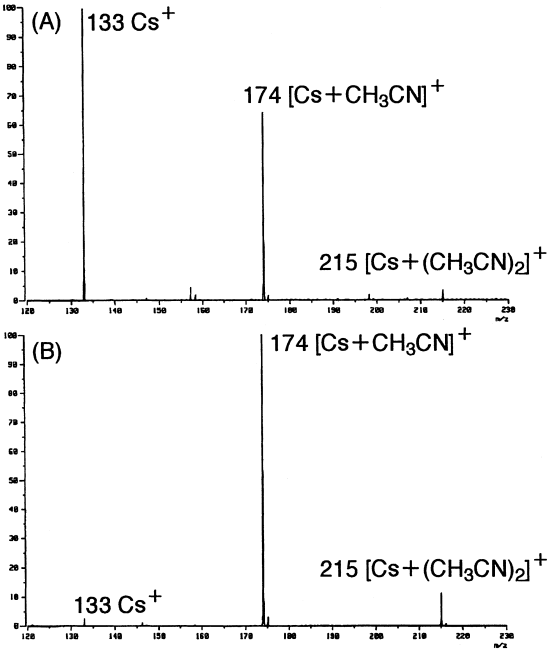

Figure 2. ESI-MS spectra of CsI in acetonitrile at different desolvation chamber temperatures: (A) 200°C and (B) 10°C.

Though desolvation by using a heated capillary and/or drying gas is thought to be an important step for ionization in the conventional ESI process,[19] we confirmed that solvation (promoting electrolytic dissociation to form molecular ions) is a critical step in the CSI process for ionic compounds. In addition, multiply charged molecular ions with solvent attached are expected to be formed in this ionization process because the solvent is also further polarized at lower temperature, promoting solvation.

Adamantanoid type Pt(II) complexes

Compound **1a**, having a large hydrophobic space, was constructed from ten molecular components including six Pt(II)(en) and four rigid tridentate ligands (Scheme 1). This molecule belongs to the category of ultrafine particles because its size reaches the nanometer scale. The structure has been definitely characterized only in the case of the guest (four adamantanoles)-encapsulating product, by means of X-ray crystallography as well as NMR spectroscopy.[1,8] Although various guest molecules can be included in the hydrophobic space of this molecule, no practical characterization procedure had been established. Therefore, we examined the characterization of these compounds by using CSI-MS.

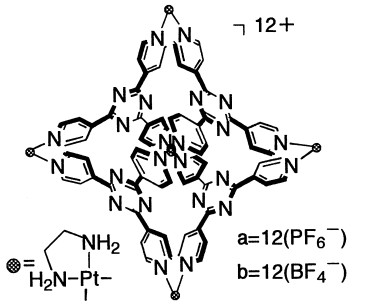

Compound **1a**: $(C_{84}H_{96}N_{36}Pt_6)^{12+} \cdot 12(PF_6^-)$

FW. 4519.98

Compound **1b**: $(C_{84}H_{96}N_{36}Pt_6)^{12+} \cdot 12(BF_4^-)$

FW. 3822.06

Scheme 1.

The CSI- and conventional ESI-MS spectra of a 0.1 mmol/L acetonitrile solution of **1a** (PF_6^- salt) were compared (Fig. 3). While a significant result was not obtained from the conventional ESI-MS (Fig. 3B), presumably because of the high desolvation plate temperature (200°C), multiply charged molecular ions of $[M-(PF_6)_n+(CH_3CN)_m]^{n+}$ (n=3–10, m=0–21) (M; monomeric molecule) were clearly observed without decomposition in the CSI-MS (Fig. 3A). Interestingly, the number of acetonitriles[28–30] (m) attached to the molecular ion increased with increasing positive charge (Fig. 4). This suggests that the acetonitrile molecules solvated the Pt^{2+} ions. Detailed assignments of ion peaks are shown in Table 1. Accurate identification of multiply charged molecular ions with bound solvent was accomplished by means of exact mass measurement using crown ether compounds {[(dibiphenyl-22-crown-6)+K]$^+$;

551.1836 and [(dinaphthyl-24-crown-8)+Na]$^+$; 571.2308} as internal calibrants[31] {[M−7(PF_6)+10AN]$^{7+}$; obs.

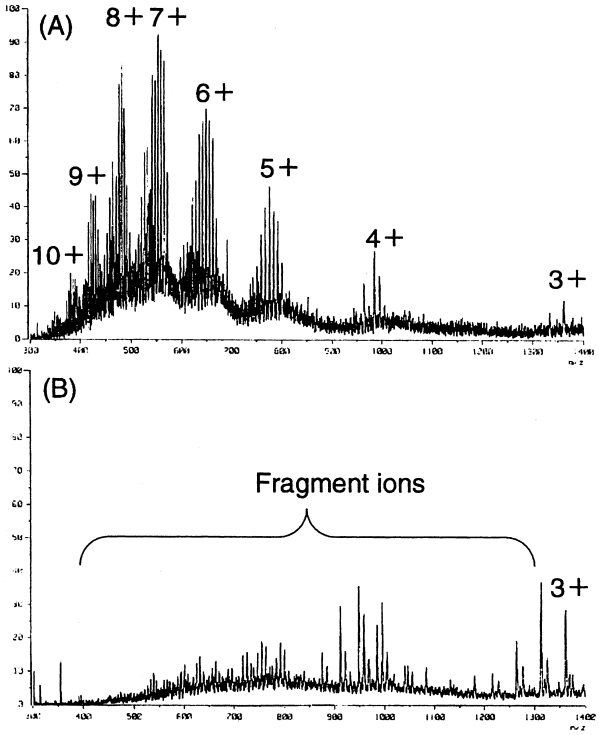

Figure 3. Spectral comparison of compound **1a** between (A) CSI and (B) ESI.

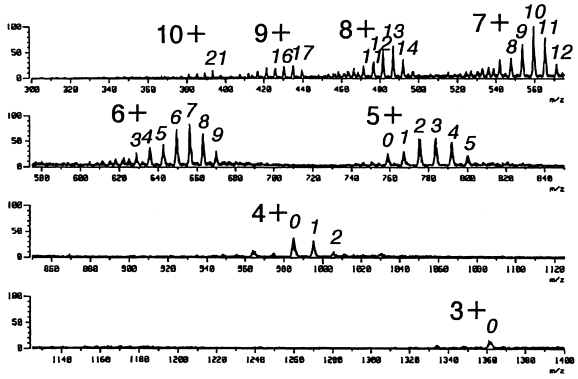

Figure 4. CSI-MS spectrum of compound **1a**. *Italic* numbering indicates the number of CH_3CN attached.

559.2507, calcd 559.2480} (Fig. 5). We also examined whether changing the counter anions would influence the intensity of the molecular ions in the CSI. The CSI-MS spectrum of compound **1b**, in which PF_6^- is replaced with BF_4^-, was measured. [K+CH_3CN]$^+$ (*m*/*z*=80), [Na+ 2CH_3CN]$^+$ (*m*/*z*=105) and the multiply charged molecular ions [M−(BF_4)$_n$+(CH_3CN)$_m$]$^{n+}$ (*n*=3–6, *m*=0–7) were again observed (Fig. 6 and Table 2). However, the intensity of the molecular ions as well as the observed ion charges were clearly reduced compared to those of **1a**. This can perhaps be ascribed to the difference of coordination ability of PF_6^- and BF_4^- to Pt^{2+}. PF_6^- seems more favorable for the CSI process based on solvation, because the lower coordination ability of this anion may promote dissociation. Selection of the counter ion seems to be important.

Table 1. Assignments of CSI-MS peaks of **1a** (M=monomer, AN=acetonitrile)

m/*z*	Molecular composition
381	[M−10(PF_6)+18AN]$^{10+}$
385	[M−10(PF_6)+19AN]$^{10+}$
389	[M−10(PF_6)+20AN]$^{10+}$
393	[M−10(PF_6)+21AN]$^{10+}$
416	[M−9(PF_6)+13AN]$^{9+}$
421	[M−9(PF_6)+14AN]$^{9+}$
426	[M−9(PF_6)+15AN]$^{9+}$
430	[M−9(PF_6)+16AN]$^{9+}$
435	[M−9(PF_6)+17AN]$^{9+}$
466	[M−8(PF_6)+9AN]$^{8+}$
471	[M−8(PF_6)+10AN]$^{8+}$
476	[M−8(PF_6)+11AN]$^{8+}$
482	[M−8(PF_6)+12AN]$^{8+}$
487	[M−8(PF_6)+13AN]$^{8+}$
492	[M−8(PF_6)+14AN]$^{8+}$
541	[M−7(PF_6)+7AN]$^{7+}$
548	[M−7(PF_6)+8AN]$^{7+}$
554	[M−7(PF_6)+9AN]$^{7+}$
559	[M−7(PF_6)+10AN]$^{7+}$
565	[M−7(PF_6)+11AN]$^{7+}$
571	[M−7(PF_6)+12AN]$^{7+}$
629	[M−6(PF_6)+3AN]$^{6+}$
636	[M−6(PF_6)+4AN]$^{6+}$
642	[M−6(PF_6)+5AN]$^{6+}$
649	[M−6(PF_6)+6AN]$^{6+}$
656	[M−6(PF_6)+7AN]$^{6+}$
663	[M−6(PF_6)+8AN]$^{6+}$
670	[M−6(PF_6)+9AN]$^{6+}$
759	[M−5(PF_6)]$^{5+}$
767	[M−5(PF_6)+AN]$^{5+}$
776	[M−5(PF_6)+2AN]$^{5+}$
784	[M−5(PF_6)+3AN]$^{5+}$
792	[M−5(PF_6)+4AN]$^{5+}$
800	[M−5(PF_6)+5AN]$^{5+}$
985	[M−4(PF_6)]$^{4+}$
995	[M−4(PF_6)+AN]$^{4+}$
1005	[M−4(PF_6)+2AN]$^{4+}$
1361	[M−3(PF_6)]$^{3+}$

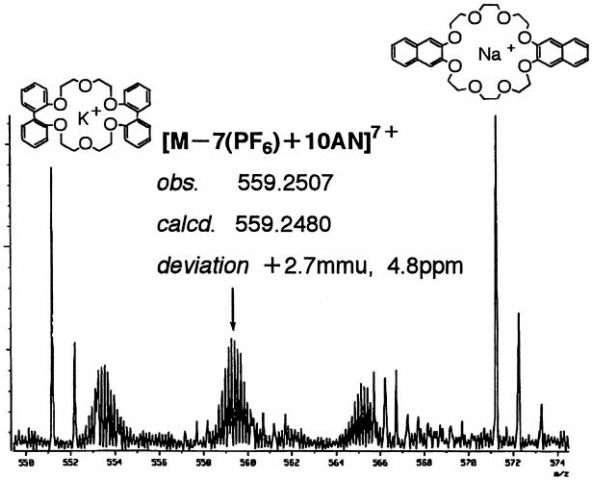

Figure 5. High-resolution CSI-MS spectrum of compound **1a** showing the exact mass number.

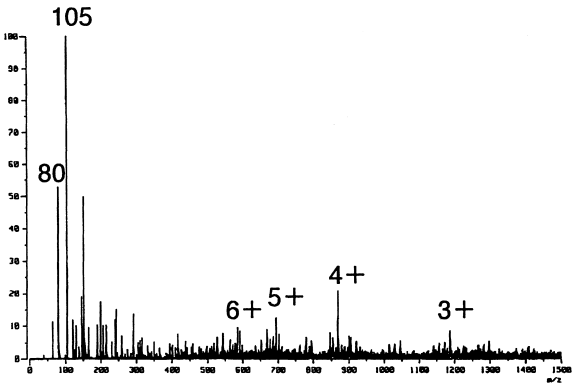

Figure 6. CSI-MS spectrum of compound **1b**.

Table 2. Assignments of CSI-MS peaks of **1b**

m/z	Molecular composition
584	$[M-6(PF_6)+5AN]^{6+}$
591	$[M-6(PF_6)+6AN]^{6+}$
598	$[M-6(PF_6)+7AN]^{6+}$
678	$[M-5(PF_6)]^{5+}$
686	$[M-5(PF_6)+AN]^{5+}$
694	$[M-5(PF_6)+2AN]^{5+}$
702	$[M-5(PF_6)+3AN]^{5+}$
710	$[M-5(PF_6)+4AN]^{5+}$
869	$[M-4(PF_6)]^{4+}$
1187	$[M-3(PF_6)]^{3+}$

Cage-like interlocking type Pt(II) complex

Compound **2** was constructed from ten molecular components including six Pt(II)(en) and two kinds of rigid tridentate ligands (Scheme 2). The molecule consists of two identical cage frameworks interlocking with each other. The structure was characterized by means of X-ray crystallography as well as NMR spectroscopy. However, the precise locations of some counter anions as well as the interlocking behavior in solution were not clarified. Mass spectrometric observation using the CSI procedure finally confirmed the structure.

An acetonitrile solution of **2** (PF_6^- salt) was subjected to CSI-MS. Multiply charged molecular ions for $[M-(PF_6)_n+(CH_3CN)_m]^{n+}$ (n=4–11, m=2–26) were clearly observed without decomposition (Fig. 7 and Table 3). The CSI-MS of the BF_4^- salt also afforded a series of ion peaks corresponding to $[M-(BF_4)_n+(CH_3CN)_m]^{n+}$. An exact mass measurement was performed by using crown ether compounds {[(dibiphenyl-22-crown-6)+K]$^+$; 551.1836 and [(dinaphthyl-24-crown-8)+K]$^+$; 587.2047} as internal calibrants {$[M-8(PF_6)+14AN]^{8+}$; obs. 559.3928, calcd. 559.3953}.

Molecular necklace type Pt(II) complex

Molecular necklaces are supramolecular species in which a number of small rings (beads) such as cucurbituril are threaded onto a large ring (string). They are topological isomers of linear oligocatenanes, in which the rings are mechanically interlocked in a linear fashion. Compound **3** was constructed from nine molecular components including three Pt(II)(en), three molecular beads and three molecular strings (Scheme 3).

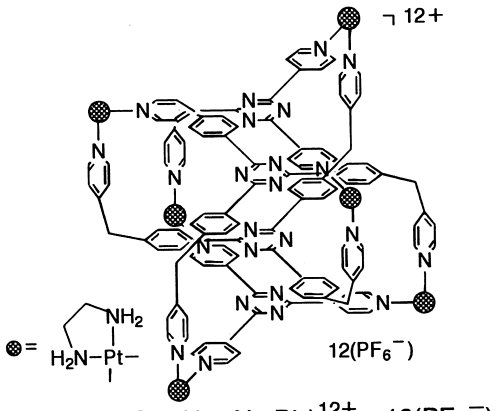

Compound **2**: $(C_{126}H_{132}N_{36}Pt_6)^{12+} \cdot 12(PF_6^-)$

FW. 5060.73

Scheme 2.

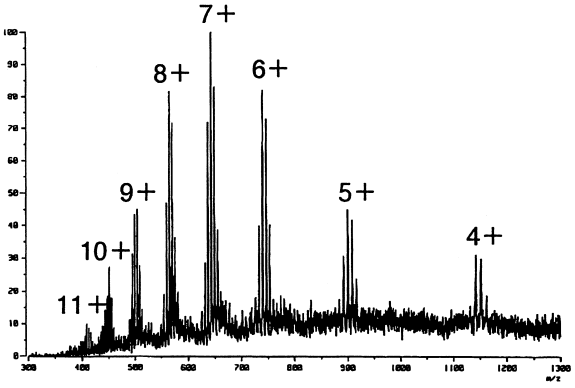

Figure 7. CSI-MS spectrum of compound **2**.

Table 3. Assignments of CSI-MS peaks of **2**

m/z	Molecular composition
408	$[M-11(PF_6)+25AN]^{11+}$
412	$[M-11(PF_6)+26AN]^{11+}$
443	$[M-10(PF_6)+20AN]^{10+}$
447	$[M-10(PF_6)+21AN]^{10+}$
451	$[M-10(PF_6)+22AN]^{10+}$
455	$[M-10(PF_6)+23AN]^{10+}$
495	$[M-9(PF_6)+17AN]^{9+}$
499	$[M-9(PF_6)+18AN]^{9+}$
504	$[M-9(PF_6)+19AN]^{9+}$
509	$[M-9(PF_6)+20AN]^{9+}$
559	$[M-8(PF_6)+14AN]^{8+}$
565	$[M-8(PF_6)+15AN]^{8+}$
570	$[M-8(PF_6)+16AN]^{8+}$
575	$[M-8(PF_6)+17AN]^{8+}$
630	$[M-7(PF_6)+9AN]^{7+}$
637	$[M-7(PF_6)+10AN]^{7+}$
642	$[M-7(PF_6)+11AN]^{7+}$
648	$[M-7(PF_6)+12AN]^{7+}$
654	$[M-7(PF_6)+13AN]^{7+}$
733	$[M-6(PF_6)+5AN]^{6+}$
739	$[M-6(PF_6)+6AN]^{6+}$
746	$[M-6(PF_6)+7AN]^{6+}$
753	$[M-6(PF_6)+8AN]^{6+}$
892	$[M-5(PF_6)+3AN]^{5+}$
900	$[M-5(PF_6)+4AN]^{5+}$
908	$[M-5(PF_6)+5AN]^{5+}$
916	$[M-5(PF_6)+6AN]^{5+}$
1141	$[M-4(PF_6)+2AN]^{4+}$
1150	$[M-4(PF_6)+3AN]^{4+}$

Multiply charged molecular ions for $[M-(PF_6)_n+(CH_3CN)_m]^{n+}$ (n=3–10, m=0–13) were clearly observed without decomposition (Fig. 8 and Table 4). The observed isotopic patterns of the ion cluster match the calculated pattern well. The structure of an extended molecular necklace of square shape having four beads[10] was also characterized by means of CSI-MS.

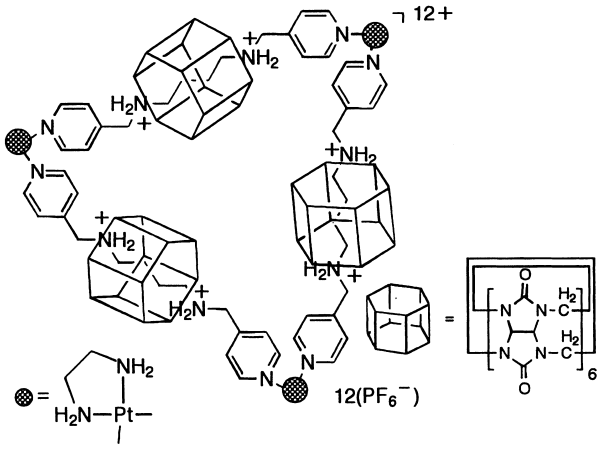

Compound **3**: $(C_{162}H_{132}N_{90}O_{36}Pt_3)^{12+} \cdot 12(PF_6^-)$

FW. 6312.79

Scheme 3.

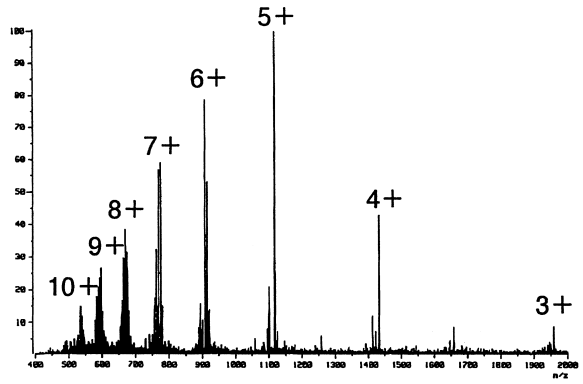

Figure 8. CSI-MS spectrum of compound **3**.

Table 4. Assignments of CSI-MS peaks of **3**

m/z	Molecular composition
532	$[M-10(PF_6)+11AN]^{10+}$
536	$[M-10(PF_6)+12AN]^{10+}$
540	$[M-10(PF_6)+13AN]^{10+}$
579	$[M-9(PF_6)+5AN]^{9+}$
588	$[M-9(PF_6)+6AN]^{9+}$
593	$[M-9(PF_6)+7AN]^{9+}$
597	$[M-9(PF_6)+8AN]^{9+}$
659	$[M-8(PF_6)+3AN]^{8+}$
665	$[M-8(PF_6)+4AN]^{8+}$
670	$[M-8(PF_6)+5AN]^{8+}$
675	$[M-8(PF_6)+6AN]^{8+}$
757	$[M-7(PF_6)]^{7+}$
763	$[M-7(PF_6)+AN]^{7+}$
769	$[M-7(PF_6)+2AN]^{7+}$
774	$[M-7(PF_6)+3AN]^{7+}$
780	$[M-7(PF_6)+4AN]^{7+}$
907	$[M-6(PF_6)]^{6+}$
914	$[M-6(PF_6)+AN]^{6+}$
921	$[M-6(PF_6)+2AN]^{6+}$
1117	$[M-5(PF_6)]^{5+}$
1433	$[M-4(PF_6)]^{4+}$
1959	$[M-3(PF_6)]^{3+}$

Molecular squares

Many molecular squares in which transition metals (*M*), hypervalent iodine[13] or organic frameworks provide the four right-angled edges of the square have been reported in recent years. We have been engaged in structural characterization of several molecular square assemblies based on $[M(en)(NO_3)_2]$ and 4,4′-bipyridine. Since X-ray crystallographic analysis is difficult because of highly disordered counter ions and solvent molecules, as well as the guest molecules, which are necessary to form a single crystal, analytical results have been difficult to obtain. CSI-MS is a promising method to carry out solution structure analyses of these compounds.

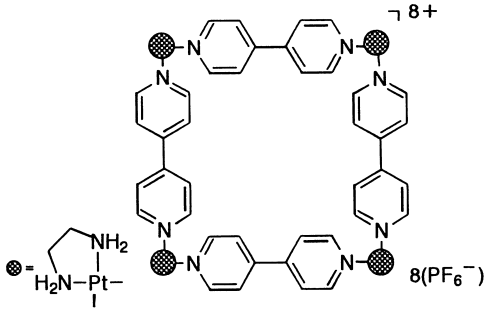

Compound **4**: $(C_{48}H_{64}N_{16}Pt_4)^{8+} \cdot 8(PF_6^-)$

FW. 2804.18

Scheme 4.

A square type Pt(II) complex, compound **4**, was constructed from eight molecular components including four Pt(II)(en) and four 4,4′-bipyridines (Scheme 4). Molecular ions for $[M-(PF_6)_n+(CH_3CN)_m]^{n+}$ (n=2–8, m=0–16) were clearly observed without decomposition (Fig. 9 and Table 5). An exact mass measurement was performed by using crown ether compounds {$[(dibenzo\text{-}18\text{-}crown\text{-}6)+Na]^+$; 383.1471 and $[(dibenzo\text{-}18\text{-}crown\text{-}6)+K]^+$; 399.1210} as internal calibrants {$[M-6(PF_6)+10AN]^{6+}$; obs. 390.9339, calcd 390.9335}.

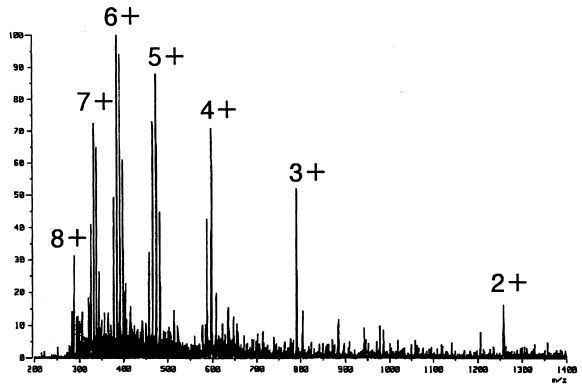

Figure 9. CSI-MS spectrum of compound **4**.

Table 5. Assignments of CSI-MS peaks of **4**

m/z	Molecular composition
283	$[M-8(PF_6)+15AN]^{8+}$
288	$[M-8(PF_6)+16AN]^{8+}$
320	$[M-7(PF_6)+11AN]^{7+}$
326	$[M-7(PF_6)+12AN]^{7+}$
332	$[M-7(PF_6)+13AN]^{7+}$
338	$[M-7(PF_6)+14AN]^{7+}$
344	$[M-7(PF_6)+15AN]^{7+}$
377	$[M-6(PF_6)+8AN]^{6+}$
384	$[M-6(PF_6)+9AN]^{6+}$
391	$[M-6(PF_6)+10AN]^{6+}$
398	$[M-6(PF_6)+11AN]^{6+}$
457	$[M-5(PF_6)+5AN]^{5+}$
465	$[M-5(PF_6)+6AN]^{5+}$
473	$[M-5(PF_6)+7AN]^{5+}$
482	$[M-5(PF_6)+8AN]^{5+}$
577	$[M-4(PF_6)+2AN]^{4+}$
587	$[M-4(PF_6)+3AN]^{4+}$
597	$[M-4(PF_6)+4AN]^{4+}$
608	$[M-4(PF_6)+5AN]^{4+}$
790	$[M-3(PF_6)]^{3+}$
803	$[M-3(PF_6)+AN]^{3+}$
817	$[M-3(PF_6)+2AN]^{3+}$
1257	$[M-2(PF_6)]^{2+}$

A square type Pd(II) complex, compound **5**, was constructed from eight molecular components including four Pd(II)(en) and four 4,4′-bipyridines (Scheme 5). The molecular structure has been roughly characterized by means of X-ray crystallography. Although the NMR spectrum[4] of compound **5** suggested a square type compound, molecular ions could not be obtained by CSI-MS using an acetonitrile solution (0.1 mmol/L).

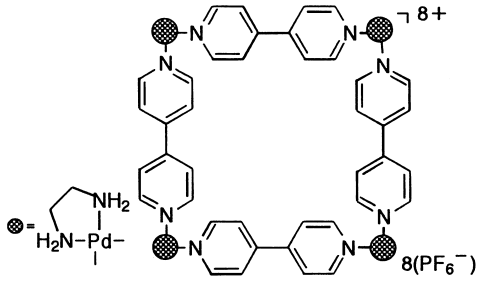

Compound **5**: $(C_{48}H_{64}N_{16}Pd_4)^{8+} \cdot 8(PF_6^-)$

FW. 2450.54

Scheme 5.

This square type Pd(II) complex may decompose when dissolved in acetonitrile at such a low concentration, due to the lower coordinatability of Pd compared to Pt. When a 4 mmol/L acetonitrile solution (comparable to the NMR experiment) was used, multiply charged molecular ions of $[M-(PF_6)_n+(CH_3CN)_m]^{n+}$ (n=2–5, m=0–8) and $[D-(PF_6)_n+(CH_3CN)_m]^{n+}$ (n=3–5, m=0–2) (D; dimeric molecule) were clearly observed in the CSI-MS (Fig. 10 and Table 6). The observed isotopic patterns of the ion cluster match the calculated pattern well for these ion peaks. Thus, two different kinds of self-assembling Pd(II) complexes, a monomer and a dimer appear to be formed in equilibrium in solution. These results show that CSI-MS is applicable to concentrated solutions of such complexes, whose framework constitution is strongly influenced by their concentration.

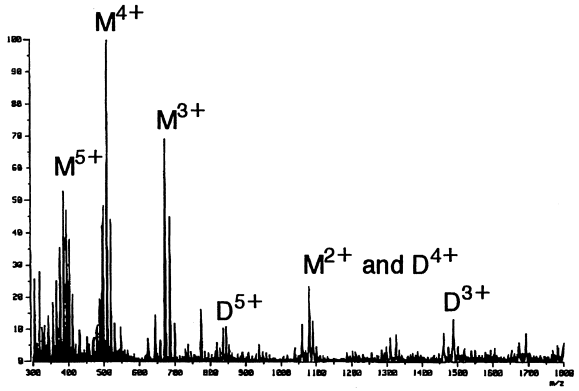

Figure 10. CSI-MS spectrum of compound **5**.

Table 6. Assignments of CSI-MS peaks of **5** (D=dimeric structure)

m/z	Molecular composition
386	$[M-5(PF_6)+5AN]^{5+}$
394	$[M-5(PF_6)+6AN]^{5+}$
402	$[M-5(PF_6)+7AN]^{5+}$
411	$[M-5(PF_6)+8AN]^{5+}$
498	$[M-4(PF_6)+3AN]^{4+}$
509	$[M-4(PF_6)+4AN]^{4+}$
519	$[M-4(PF_6)+5AN]^{4+}$
672	$[M-3(PF_6)]^{3+}$
685	$[M-3(PF_6)+AN]^{3+}$
699	$[M-3(PF_6)+2AN]^{3+}$
835	$[D-5(PF_6)]^{5+}$
843	$[D-5(PF_6)+AN]^{5+}$
852	$[D-5(PF_6)+2AN]^{5+}$
1080	$[M-2(PF_6)]^{2+}$ $[D-4(PF_6)+7AN]^{4+}$
1090	$[D-4(PF_6)+AN]^{4+}$
1489	$[D-3(PF_6)]^{3+}$

A square type Pd(II)–Ru(II) complex, compound **6**, was constructed from eight molecular components including two Pd(II)(en), two Ru(II)(di-2,2′-bipyridine) and four 4,4′-bipyridines (Scheme 6). The CSI-MS spectrum was observed with a 4 mmol/L acetonitrile solution.

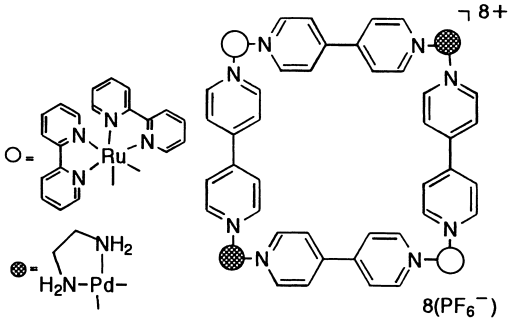

Compound **6**: $(C_{80}H_{80}N_{20}Pd_2Ru_2)^{8+} \cdot 8(PF_6^-)$

FW. 2944.39

Scheme 6.

Multiply charged molecular ions of $[M-(PF_6)_n+(CH_3CN)_m]^{n+}$ (n=2–6, m=0–4) together with $[D-(PF_6)_n]^{n+}$ (n=4–5) were clearly observed in the CSI-MS (Fig. 11). An exact mass measurement was performed by using crown ether compounds {[(dibenzo-24-crown-

8)+Cs]$^+$; 581.1152 and [(di-*t*-butylbenzo-18-crown-6)+Cs]$^+$; 605.1879} as internal calibrants {[M−4(PF$_6$)]$^{4+}$; obs. 591.0420, calcd. 591.0414}. Dimeric molecular ions of [D−(PF$_6$)$_n$]$^{n+}$ (n=4–5) were also observed in the spectrum (Fig. 11 and Table 7). An interesting property of the solvent attachment in the CSI process is apparent from a comparison of **5** and **6**. The solvation ability of **5** is clearly superior to that of **6**. This may be related to the bulkiness of the ligands. That is, a greater number of CH_3CN was attached to the molecular ion in **5** as compared to **6**, in which a couple of bulky ligands are coordinated to Ru. Consequently, approach of solvent molecules to the central metal may be hindered in **6**.

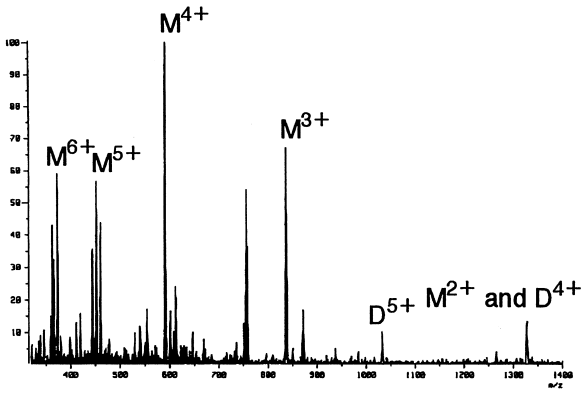

Figure 11. CSI-MS spectrum of compound **6**.

Table 7. Assignments of CSI-MS peaks of **6**

m/z	Molecular composition
366	[M−6(PF$_6$)+3AN]$^{6+}$
373	[M−6(PF$_6$)+4AN]$^{6+}$
444	[M−5(PF$_6$)]$^{5+}$
452	[M−5(PF$_6$)+AN]$^{5+}$
460	[M−5(PF$_6$)+2AN]$^{5+}$
591	[M−4(PF$_6$)]$^{4+}$
836	[M−3(PF$_6$)]$^{3+}$
1032	[D−5(PF$_6$)]$^{5+}$
1327	[M−2(PF$_6$)]$^{2+}$
	[D−4(PF$_6$)]$^{4+}$

Multiple-link interlocking type Cu(I)–Pd(II) complex

A catenane incorporating copper(I) and palladium(II) as assembling centers was synthesized. The structure of this catenane (compound **7**) was determined by means of NMR spectroscopy. This compound contains 1,10-phenanthroline and pyridine units as ligands, and one Cu(I) and two Pd(II) as the assembling template. It is anticipated that 1,10-phenanthroline coordinates to Cu(I) and the pyridine rings interact with Pd(II), constructing a [2]catenane (Scheme 7).

However, the CSI-MS spectrum of compound **7** at high concentration (4.2 mg/1 mL in CH_3CN) exhibited dimeric (D) (Cu/Pd/Ligand=2:4:4) {[D−(PF$_6$)$_n$+(CH$_3$CN)$_m$]$^{n+}$ (n=3–5, m=0–1)} and tetrameric (T) (Cu/Pd/Ligand=4:8:8) {[T−(PF$_6$)$_n$]$^{n+}$ (n=4–5)} states in equilibrium. The observed mass numbers and isotopic patterns of the ion clusters as well as the ion charges match the theoretical values well (Fig. 12A and Table 8). In the case of diluted solution (×20), the ion peaks of the tetramer disappeared and multiply charged dimer ions of [D−(PF$_6$)$_n$+(CH$_3$CN)$_m$]$^{n+}$ (n=3–7, m=0–8) were observed in CSI-MS (Fig. 12B and Table 8). The ion peaks of the dimer diminished and a new ion peak (m/z=825) formed by decomposition appeared in further diluted solution (×40) (Fig. 12C and Table 8). In even more diluted solution (×120), the ion peaks of the

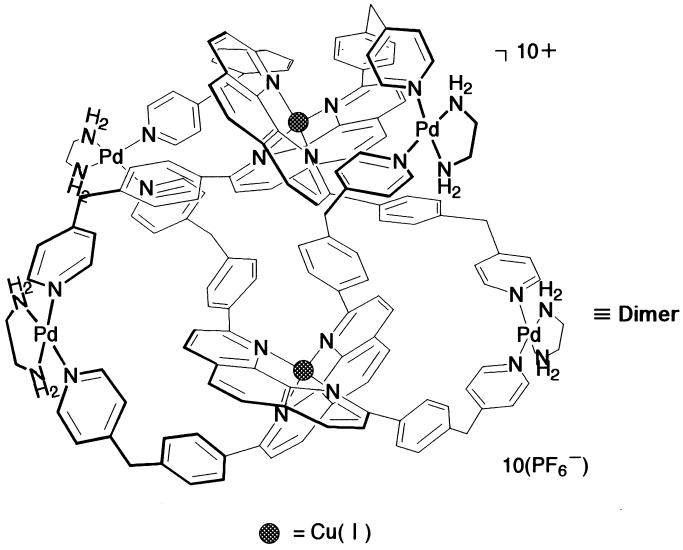

Compound **7**

(Monomer): $(C_{76}H_{68}CuN_{12}Pd_2)^{5+} \cdot 5(PF_6^-)$, FW. 2150.66

(Dimer): $(C_{152}H_{136}Cu_2N_{24}Pd_4)^{10+} \cdot 10(PF_6^-)$, FW. 4301.32

(Tetramer): $(C_{304}H_{272}Cu_4N_{48}Pd_8)^{20+} \cdot 20(PF_6^-)$, FW. 8602.64

Scheme 7.

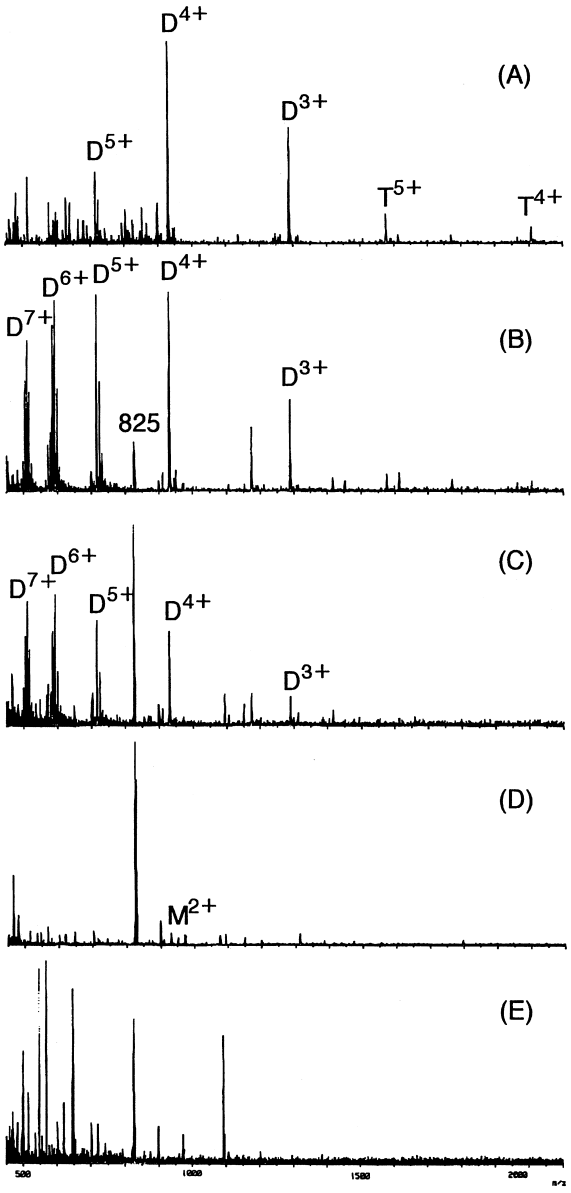

Figure 12. CSI-MS spectra of compound **7** at various concentrations: (A) 4.2 mg/1 mL; (B) ×20, (C) ×40, (D) ×120 and (E) ×200.

Table 8. Assignments of CSI-MS peaks of **7** (T=tetramer)

m/*z*	Molecular composition
505	$[D-7(PF_6)+6AN]^{7+}$
511	$[D-7(PF_6)+7AN]^{7+}$
516	$[D-7(PF_6)+8AN]^{7+}$
572	$[D-6(PF_6)]^{6+}$
579	$[D-6(PF_6)+AN]^{6+}$
586	$[D-6(PF_6)+2AN]^{6+}$
592	$[D-6(PF_6)+3AN]^{6+}$
599	$[D-6(PF_6)+4AN]^{6+}$
715	$[D-5(PF_6)]^{5+}$
723	$[D-5(PF_6)+AN]^{5+}$
930	$[D-4(PF_6)]^{4+}$
	$[M-2(PF_6)]^{2+}$
1288	$[D-3(PF_6)]^{3+}$
1575	$[T-5(PF_6)]^{5+}$
2005	$[T-4(PF_6)]^{4+}$

monomeric constitution $[M-(PF_6)_2]^{2+}$ as well as fragment ions generated by decomposition were observed, while the ion peaks of the dimer completely disappeared (Fig. 12D and Table 8). The change from dimeric to monomeric structure depending on the concentration is clearly observed in the different charge ratios of 4+ and 2+ at an identical ion peak (*m*/*z*=930) (Fig. 13). Finally, no significant ion peak other than fragment ions was observed in highly diluted solution (×200), suggesting disassembly of this compound (Fig. 12E). Thus, CSI-MS was proved to be a powerful tool for analyzing the equilibria of multiple-link self-assembling catenanes in solution.

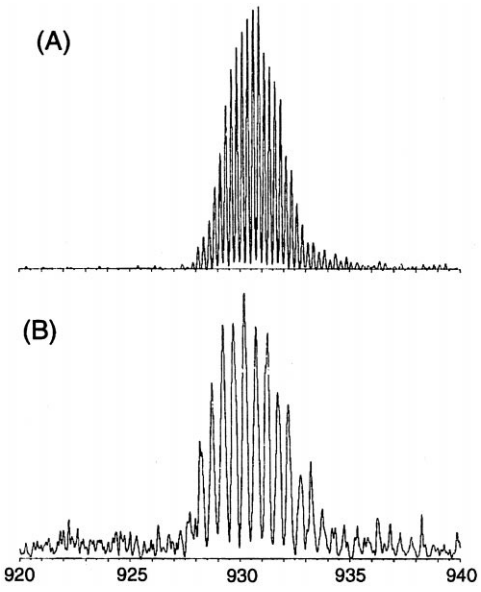

Figure 13. The isotopic patterns of 930 (*m*/*z*): (A) dimer (4+) and (B) monomer (2+).

Tubular type Pd(II) complexes

The tubular structures of compounds **8a**, **8b** and **8c** were constructed by the assembly of oligo(3,4-pyridine)s by linking them through Pd(II) (Scheme 8). The guest molecule (4,4′-biphenylene-dicarboxylate) was necessary for their formation. It is suggested that as soon as the tubular type Pd(II) complex assembled with a guest molecule is dissolved in even a small amount of an organic solvent such as acetonitrile and methanol, the guest molecule will be removed from the hydrophobic space inside in the compound, resulting in decomposition of the tubular framework itself. That is, these compounds are stable only in aqueous solution.

When a 3 mmol/L aqueous solution of compound **8a** was used and the temperature of the desolvation chamber was in the range of 0–10°C, multiply charged molecular ions of $[M-(NO_3)_n]^{n+}$ (n=4–6) were seen. Molecular ions were not observed at a desolvation chamber temperature of more than 15°C (Fig. 14A and Table 9). The molecular structures of other tubular type Pd(II) complexes were also analyzed by means of CSI-MS. $[M-(NO_3)_n]^{n+}$ (n=3–5) and $[M-(NO_3)_n]^{n+}$ (n=3–4) were observed for **8b** and **8c**, respectively (Fig. 14 and Table 9). These

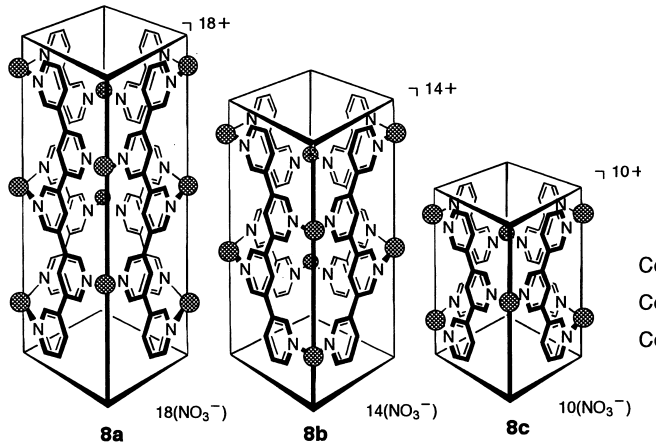

Guest = O^-OC–⟨⟩–COO^-

Compound **8a**: $(C_{134}H_{156}N_{40}O_4Pd_{10})^{18+} \cdot 18(NO_3^-)$, FW. 4571.23

Compound **8b**: $(C_{110}H_{128}N_{32}O_4Pd_8)^{14+} \cdot 14(NO_3^-)$, FW. 3681.87

Compound **8c**: $(C_{86}H_{100}N_{24}O_4Pd_6)^{10+} \cdot 10(NO_3^-)$, FW. 2792.47

Scheme 8.

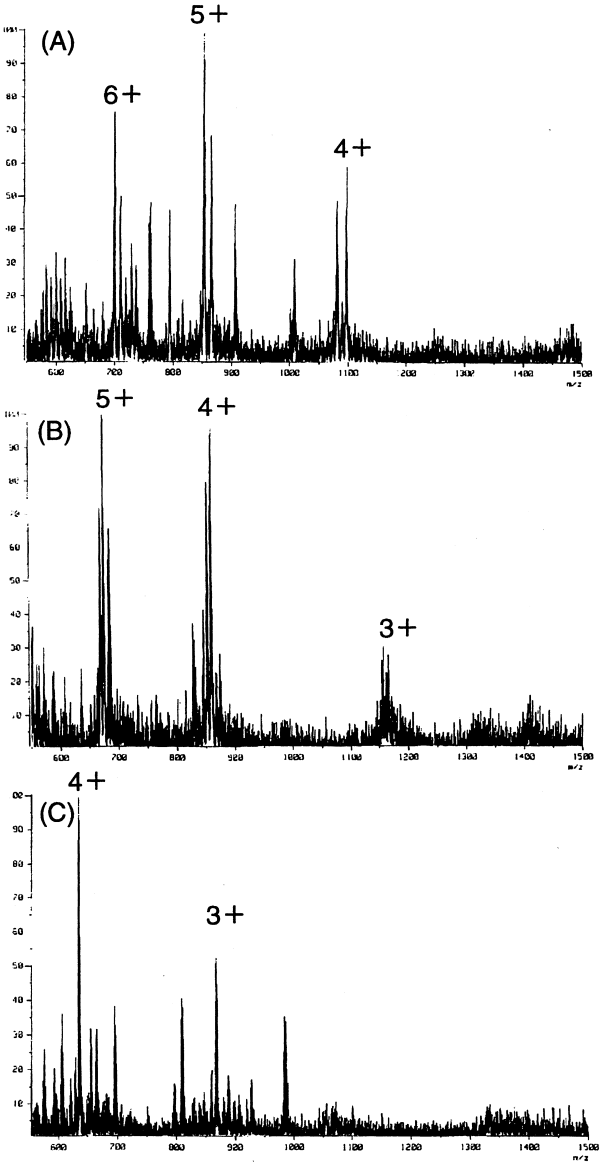

Figure 14. CSI-MS spectra of (A) compound **8a**, (B) compound **8b** and (C) compound **8c**.

Table 9. Assignments of CSI-MS peaks of **8a**–**c**

Compound	*m/z*	Molecular composition
8a	700	$[M-6(NO_3)]^{6+}$
	852	$[M-5(NO_3)]^{5+}$
	1081	$[M-4(NO_3)]^{4+}$
	1097	$[M-4(NO_3)+HNO_3]^{4+}$
8b	674	$[M-5(NO_3)]^{5+}$
	858	$[M-4(NO_3)]^{4+}$
	1165	$[M-3(NO_3)]^{3+}$
8c	636	$[M-4(NO_3)]^{4+}$
	869	$[M-3(NO_3)]^{3+}$

molecular ion peaks also disappeared at temperatures above 15°C in the desolvation chamber. In the case of aqueous solution, the molecular ions could be clearly observed by adjusting the temperature of the desolvation chamber to near the freezing point of water.

Conclusions

The coldspray ionization apparatus has been developed and applied to characterize several self-assembling nano-sized metal complexes. Moreover, we accomplished exact mass measurements of molecular ions using crown ether compounds as internal standards. The results may be summarized as follows: (1) Multiply charged molecular ions solvated with many acetonitrile molecules were observed in acetonitrile solution. (2) Pd(II) complex structures in highly concentrated solutions could be characterized and dimeric molecular ions were observed. (3) Multiple-link self-assembling catenanes in an equilibrium state in solution could be analyzed. (4) The molecular ions were clearly observed by adjusting the temperature of the desolvation chamber to near the freezing point of water in the case of aqueous solutions. Although the mechanism of CSI is still under investigation, we anticipate that ionization is promoted by the electrolytic dissociation based on increased polarizability of the compound owing to the higher dielectric constant at low temperature, which also reduces thermal decomposition of the analyte. CSI-MS

should be applicable to a wide variety of labile ionic compounds.

Experimental

Typical measurement conditions are as follows: acceleration voltage; 5.0 kV, needle voltage; 2.5 kV, needle current; 350–700 nA, orifice voltage; 20–70 V, resolution (10% valley definition); 5000, sample flow; 10 μL/min, solvent; acetonitrile or aq., concentration; 0.01–0.1 mmol/L; spray temperature, −20°C; ion source temperature, −50–15°C.

Self-assembling nano-sized metal complexes, adamantanoid type Pt(II) complexes (**1**),[1] cage-like interlocking type Pt(II) complex (**2**),[2]molecular necklace type Pt(II) complex (**3**),[3] square type Pt(II) complex (**4**),[4,5] square type Pd(II) complex (**5**),[4,5] square type Pd(II)–Ru(II) complex (**6**), multiple-link interlocking type Cu(I)–Pd(II) complex (**7**)[6] and tubular type Pd(II) complexes (**8**)[7] were prepared for CSI-MS measurement by using general methods described in the literature.[1–7]

References

1. Fujita, M.; Oguro, D.; Miyazawa, M.; Oka, H.; Yamaguchi, K.; Ogura, K. *Nature* **1995**, *378*, 469–471.
2. Fujita, M.; Fujita, N.; Ogura, K.; Yamaguchi, K. *Nature* **1999**, *400*, 52–55.
3. Whang, D.; Park, K.-M.; Heo, J.; Ashton, P.; Kim, K. *J. Am. Chem. Soc.* **1998**, *120*, 4899–4900.
4. Fujita, M.; Yazaki, J.; Ogura, K. *J. Am. Chem. Soc.* **1990**, *112*, 5645–5646.
5. Fujita, M.; Sasaki, O.; Mitsuhashi, T.; Yamaguchi, K.; Ogura, K. *J. Chem. Soc., Chem. Commun.* **1996**, 1535–1536.
6. Ibukuro, F.; Fujita, M.; Yamaguchi, K.; Sauvage, J.-P. *J. Am. Chem. Soc.* **1999**, *121*, 11014–11015.
7. Aoyagi, M.; Biradha, K.; Fujita, M. *J. Am. Chem. Soc.* **1999**, *121*, 7457–7458.
8. Ibukuro, F.; Kusukawa, T.; Fujita, M. *J. Am. Chem. Soc.* **1998**, *120*, 8561–8562.
9. Takada, N.; Umemoto, K.; Yamaguchi, K.; Fujita, M. *Nature* **1999**, *398*, 79–81.
10. Roh, S.-G.; Park, K.-M.; Park, G.-J.; Sakamoto, S.; Yamaguchi, K.; Kim, K. *Angew. Chem., Int. Ed. Engl.* **1999**, *38*, 638–641.
11. Ikeda, A.; Yoshimura, M.; Udzu, H.; Fukuhara, C.; Shinkai, S. *J. Am. Chem. Soc.* **1999**, *121*, 4296–4297.
12. Bitsch, F.; Hegy, G.; Dietrich-Buchecker, C.; Leize, E.; Sauvage, J.-P.; Dorsselaer, A. V. *J. Am. Chem. Soc.* **1991**, *113*, 4023–4025.
13. Whiteford, J. A.; Rachlin, E. M.; Stang, P. J. *Angew. Chem., Int. Ed. Engl.* **1996**, *35*, 2524–2529.
14. Anderson, U. N.; Konig, S.; Leary, J. A.; Freitas, M.; Marshall, A. G. *J. Am. Soc. Mass Spectrom.* **1999**, 352–354.
15. Wilson, S. R.; Perez, J.; Pasternak, A. *J. Am. Chem. Soc.* **1993**, *115*, 1994–1997.
16. Jiang, C.; Henderson, W.; Andy Hor, T. S.; McCaffrey, L. J.; Yan, Y. K. *Chem. Commun.* **1998**, 2029–2030.
17. Feichtinger, D.; Plattner, D. A.; Chen, P. *J. Am. Chem. Soc.* **1998**, *120*, 7125–7126.
18. Fenn, J. B.; Mann, M.; Meng, K.; Wong, S. F.; Whitehouse, C. M. *Science* **1989**, *246*, 64–71.
19. Kebarle, P.; Tang, L. *Anal. Chem.* **1993**, *65*, 972A–986A.
20. Yamaguchi, K.; Sakamoto, S.; Tsuruta, H.; Imamoto, T. *Chem. Commun.* **1998**, 2123.
21. Bruins, A. P. *J. Chromatogr., A* **1998**, *794*, 345–357.
22. Shiea, J.; Wang, W.-S.; Wang, C.-H.; Chen, P.-S.; Chou, C.-H. *Anal. Chem.* **1996**, *68*, 1062–1066.
23. Kim, J.; Dong, Y.; Larka, E.; Que Jr., L. *Inorg. Chem.* **1996**, *35*, 2369–2372.
24. Wang, C.-H.; Huang, M.-W.; Lee, C.-Y.; Chei, H.-L.; Huang, J.-P.; Shiea, J. *J. Am. Soc. Mass Spectrom.* **1998**, 1168–1174.
25. Blades, A. T.; Jayaweera, P.; Ikonomou, M. G.; Kebarle, P. *J. Chem. Phys.* **1990**, *92*, 5900–5906.
26. Blades, A. T.; Klassen, J. S.; Kebarle, P. *J. Am. Chem. Soc.* **1996**, *118*, 12437–12442.
27. Deng, H.; Kebarle, P. *J. Am. Chem. Soc.* **1998**, *120*, 2925–2931.
28. Henderson, W.; Nicholson, B. K. *J. Chem. Soc., Chem. Commun.* **1995**, 2531–2532.
29. Arakawa, R.; Tachibayashiki, S.; Matuo, T. *Anal. Chem.* **1995**, *67*, 4133–4138.
30. Blanchard, S.; Clainche, L. L.; Rager, M. -N.; Chansou, B.; Tuchagues, J. -P.; Duprat, A. F.; Mest, Y. L.; Reinaud, O. *Angew. Chem., Int. Ed. Engl.* **1998**, *37*, 2732–2735.
31. Yamaguchi, K.; Sakamoto, S.; Imamoto, T.; Ishikawa, T. *Anal. Sci.* **1999**, *15*, 1037–1038.